JACS JOURNAL OF THE AMERICAN CHEMICAL SOCIETY
Article
pubs.acs.org/JACS

Main-Chain Optically Active Riboflavin Polymer for Asymmetric Catalysis and Its Vapochromic Behavior

Hiroki Iida, Soichiro Iwahana, Tomohisa Mizoguchi, and Eiji Yashima*

Department of Molecular Design and Engineering, Graduate School of Engineering, Nagoya University, Nagoya 464-8603, Japan

Ⓢ *Supporting Information*

ABSTRACT: A novel optically active polymer consisting of riboflavin units as the main chain (poly-**1**) was prepared from naturally occurring riboflavin (vitamin B_2) in three steps. The riboflavin residues of poly-**1** were converted to 5-ethylriboflavinium cations (giving poly-**2**), which could be reversibly transformed into the corresponding 4a-hydroxyriboflavins (giving poly-**2OH**) through hydroxylation/dehydroxylation reactions. This reversible structural change was accompanied by a visible color change along with significant changes in the absorption and circular dichroism (CD) spectra. The nuclear Overhauser effect spectroscopy (NOESY) and CD spectra of poly-**2** revealed a supramolecularly twisted helical structure with excess one-handedness through face-to-face stacking of the intermolecular riboflavinium units, as evidenced by the apparent NOE correlations between the interstrand riboflavin units and intense Cotton effects induced in the flavinium chromophore regions. The hydroxylation of poly-**2** at the 4a-position proceeded in a diastereoselective fashion via chirality transfer from the induced supramolecular helical chirality assisted by the ribityl pendants, resulting in a 83:17 diastereomeric mixture of poly-**2OH**. The diastereoselectivity of poly-**2** was remarkably higher than that of the corresponding monomeric model (64.5:35.5), indicating amplification of the chirality resulting from the supramolecular chirality induced in the stacked poly-**2** backbones. The optically active poly-**2** efficiently catalyzed the asymmetric organocatalytic oxidation of sulfides with hydrogen peroxide, yielding optically active sulfoxides with up to 60% enantiomeric excess (ee), whose enantioselectivity was higher than that catalyzed by the monomeric counterpart (30% ee). In addition, upon exposure to primary and secondary amines, poly-**2** exhibited unique high-speed vapochromic behavior arising from the formation of 4a-amine adducts in the film.

■ INTRODUCTION

Riboflavin, well-known as vitamin B_2, plays a central role in biological systems as a redox-active unit of cofactors, such as flavin mononucleotide (FMN) and flavin adenine dinucleotide (FAD).[1] Riboflavin consists of a planar heterocyclic isoalloxazine ring with an optically active ribityl unit and affords attractive diverse functions, such as redox activity, photosensitivity, and catalytic activity.[1−3] In particular, the flavin analogues have recently received growing attention as unique and environmentally friendly organocatalysts that mimic the enzymatic processes performed by hepatic microsomal FAD-containing monooxygenase (FADMO).[3] Bruice and co-workers performed the earliest mechanistic investigation of the synthetic flavin-mediated monooxygenation and discovered that the oxidatively active 5-ethyl-4a-hydroperoxyflavin generated from the corresponding flavinium cation with hydrogen peroxide (H_2O_2) promotes the stoichiometric oxidation of sulfides and amines.[1b,4] Murahashi et al.[5] gave the first report of a flavin-catalyzed oxidation, in which 5-ethyl-4a-hydroperoxyflavin generated in situ in the presence of H_2O_2 catalytically oxidizes sulfides and amines. Since their pioneering studies, a variety of flavin-[6] and riboflavin-based organocatalysts[7] have been developed for diverse transformation reactions, including the oxidation of sulfides and amines,[6a,b,d,e,g−i,k−r,t,7b,d] Baeyer−Villiger oxidation of ketones,[6c,f,p,7a] Dakin oxidation of arylaldehydes,[6u] and hydrogenation of alkenes and alkynes with hydrazine.[6j,s,7b−e] In most cases, however, the isoalloxazine and alloxazine units of these flavin-based catalysts were synthesized through multistep procedures, and riboflavin-based organocatalysts[7] readily derived from commercially available riboflavin are still rare in spite of their economical and environmental advantages.[8] In addition, flavin-catalyzed asymmetric transformations have been limited to a few examples using artificially synthesized flavin catalysts with planar chirality[6a,b,f,o] or bearing a chiral alkyl group,[6p] for which the enantioselectivities were modest (54−74% ee) and low (<5% ee), respectively. As an exceptional example, artificial alloxazine catalysts bearing an α- or β-cyclodextrin unit that mediate the asymmetric oxidation of sulfides and give high enantioselectivity (up to 91% ee) have recently been reported.[6r,t]

On the other hand, riboflavin-containing polymers are extremely attractive and interesting not only as polymeric flavoenzyme models[9,10] but also as a new class of functional chiral materials. In particular, if macromolecular helicity and/or

Received: June 24, 2012
Published: August 15, 2012

dx.doi.org/10.1021/ja306159t | *J. Am. Chem. Soc.* 2012, 134, 15103−15113

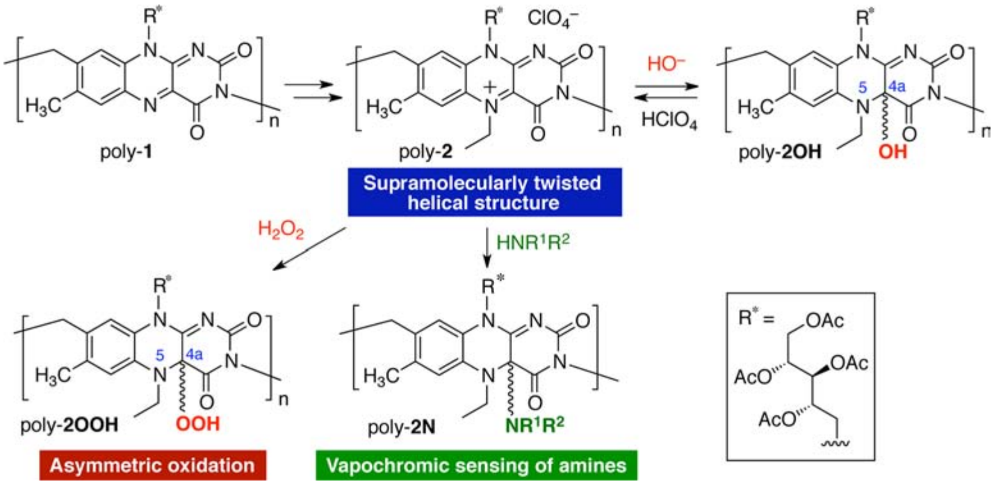

Figure 1. Optically active riboflavin-containing polymers.

Scheme 1. Synthesis of Poly-1, Poly-2, and Poly-2OH from Riboflavin

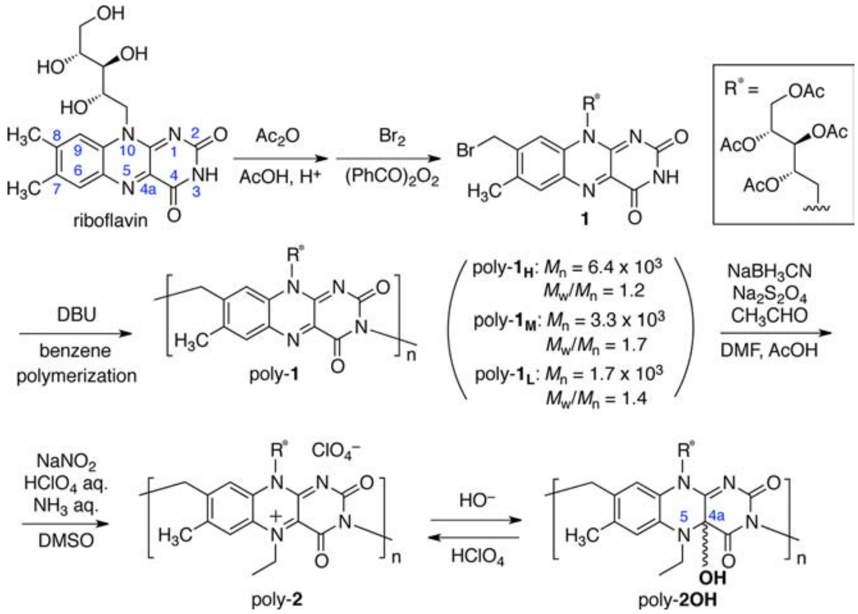

supramolecular chirality could be generated in the polymer backbone via induction by the optically active ribityl pendants, intriguing reversible chiroptical changes originating from electron transfer processes of the riboflavin units as well as asymmetric catalytic activity and chiral recognition ability might be significantly promised. However, optically active riboflavin-containing polymers are quite rare,[10] and their application as chiral materials on the basis of the chirality of the riboflavin has scarcely been reported.[11]

We recently reported the first example of a riboflavin-bound helical polymer consisting of a chromophoric polyacetylene backbone with pendant optically active riboflavin residues, which showed characteristic induced circular dichroism (ICD) in the π-conjugated polymer backbone regions due to a preferred-handed helical conformation induced by the optically active ribityl groups.[10f] The polymer also exhibited unique redox-triggered switching of the helical chirality in response to electron transfer events occurring at remote riboflavin pendants, thus showing a reversible change in its circular dichroism (CD) spectral pattern.

In the present study, we synthesized a novel optically active, riboflavin-containing polymer composed of riboflavin units as the main chain (poly-**1**). The riboflavin residues of poly-**1** were converted into 5-ethylriboflavinium cations (giving poly-**2**), which could be reversibly transformed into the corresponding 4a-hydroxyriboflavins (giving poly-**2OH**) (Figure 1). We found that the cationic poly-**2** self-assembled in solution to form a supramolecularly twisted helical structure through face-to-face stacking of the riboflavinium units, thereby showing an intense Cotton effect in the riboflavinium chromophore regions. In addition, the chirally self-assembled poly-**2** enantioselectively catalyzed the asymmetric oxidation of sulfides in the presence of H_2O_2 through the generation of oxidatively active 4a-hydroperoxyriboflavins (giving poly-**2OOH**) with higher enantioselectivity than in the reaction catalyzed by the monomeric counterpart. The mechanism and origin of this remarkable enhancement of the enantioselectivity relative to the monomeric model were thoroughly investigated by absorption, CD, and NMR spectroscopies. Furthermore, we found that poly-**2** in the film state exhibited a rapid, reversible colorimetric response to primary and secondary amine vapors resulting from the generation of 4a-amine adducts (giving poly-**2N**), thereby enabling direct visual detection of the amines. The present polymers are, to the best of our knowledge, the first examples of optically active polymers bearing riboflavin residues as the main chain.

■ RESULTS AND DISCUSSION

Synthesis of the Riboflavin-Containing Polymers and Their Chiroptical Properties. Poly-**1** was prepared by base-mediated polycondensation of 8α-bromoriboflavin (**1**) according to Scheme 1; **1** had been readily prepared from commercially available riboflavin via a two-step reaction.[13] We optimized the polymerization conditions (Table S1 in the Supporting Information) and found that the polymerization of **1** in the presence of 1 equiv of 1,8-diazabicyclo[5.4.0]undec-7-ene (DBU) in benzene produced poly-**1** in a relatively higher yield (64%), although the molecular weight (MW) was rather low because the polymer precipitated during the polymerization; the number-average molecular weight (M_n) and its distribution (M_w/M_n) as determined by size-exclusion chromatography (SEC) with poly(ethylene oxide) and poly(ethylene glycol) standards were 2.0×10^3 and 1.8, respectively. When **1** was polymerized in the presence of DBU (1 equiv) and $Bu_4N^+I^-$ (1 equiv), higher-MW poly-**1** ($M_n = 5.2 \times 10^3$, $M_w/M_n = 1.3$) was obtained in 37% yield. Therefore, the poly-**1** ($M_n = 2.0 \times 10^3$, $M_w/M_n = 1.8$) was fractionated by SEC into three fractions: a high-MW part [poly-$\mathbf{1_H}$, $M_n = 6.4 \times 10^3$, $M_w/M_n = 1.2$, degree of polymerization (DP) = 11.8], a medium-MW part (poly-$\mathbf{1_M}$, $M_n = 3.3 \times 10^3$, $M_w/M_n = 1.7$, DP = 6.1), and a low-MW part (poly-$\mathbf{1_L}$, $M_n = 1.7 \times 10^3$, $M_w/M_n = 1.4$, DP = 3.1). The DP values for poly-$\mathbf{1_H}$, poly-$\mathbf{1_M}$, and poly-$\mathbf{1_L}$ as estimated by SEC were in good agreement with those estimated by ^1H NMR analysis (10.1, 5.5, and 3.0, respectively; Figure S1 in the Supporting Information).

We then investigated the effect of the MW of poly-**1** on its chiroptical properties by measuring its CD and absorption spectra in *N*,*N*-dimethylformamide (DMF) (Figure 2). A monomeric model compound, model-**1** (see Scheme 2), was also prepared for comparison,[10f] and it showed typical absorption signals centered at around 340 and 440 nm assigned to the conjugated flavin ring chromophore[14] and weak Cotton effects in these regions. In contrast, the poly-**1** fractions exhibited intense Cotton effects in the flavin chromophore regions accompanied by a large red shift in the longer-wavelength absorption band, indicating macromolecular or supramolecular chirality that was most likely induced in the poly-**1** backbones through chirality transfer from the optically active ribityl pendants. The CD intensities of the first Cotton effects of the poly-**1** fractions in the long-wavelength absorption regions tended to increase with increasing MW in going from poly-$\mathbf{1_L}$ to poly-$\mathbf{1_M}$ and poly-$\mathbf{1_H}$, while the CD intensities and patterns of poly-$\mathbf{1_M}$ and poly-$\mathbf{1_H}$ were almost identical.

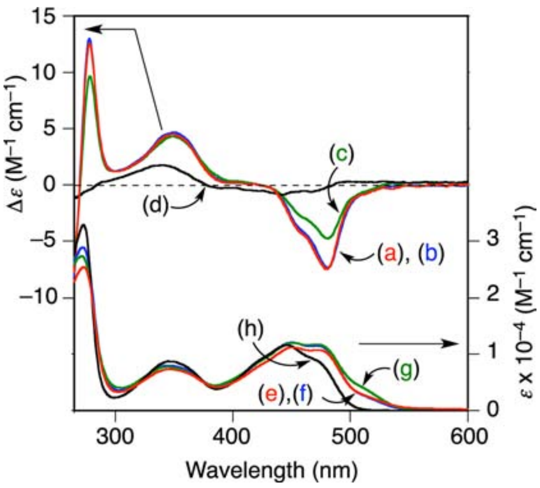

Figure 2. (a−d) CD and (e−h) absorption spectra of (a, e) poly-$\mathbf{1_H}$, (b, f) poly-$\mathbf{1_M}$, (c, g) poly-$\mathbf{1_L}$, and (d, h) model-**1** in DMF at ca. 25 °C. The concentrations were 0.5 mM.

To gain insight into the enhancement of the ICD observed in the poly-**1** fractions, the temperature- and concentration-dependent CD spectral changes were then measured for poly-$\mathbf{1_M}$. The CD intensities of poly-$\mathbf{1_M}$ in DMF increased monotonically with decreasing temperature, and its CD spectral pattern was maintained, but with a slight change in the absorption spectra (Figure S2 in the Supporting Information). The temperature-dependent CD and absorption spectral changes were reversible. Depending on the concentration (0.01−5 mM), the CD intensity also varied slightly (Figure S3 in the Supporting Information); the CD magnitude gradually increased with increasing polymer concentration, accompanied by a slight increase in the absorption.[15] Poly-$\mathbf{1_M}$ displayed an apparent emission with a peak at around 540 nm upon excitation at 450 nm in DMF (5 μM), but its intensity was approximately one-third of that of model-**1** (Figure S4 in the Supporting Information). The main chain of the polymer is not fully π-conjugated because of the methylene linkers, and therefore, this fluorescence quenching phenomenon may indicate a possible intermolecular energy transfer between the pendant fluorescent flavin residues of different polymer chains. These results suggest that the poly-**1** may form chiral aggregates in solution,[16] although the exact structure remains unclear, but the chirality of the optically active ribityl pendants appears to be transferred to induce such a supramolecular chirality.[17,18]

Next, the riboflavin residues of poly-$\mathbf{1_H}$ and poly-$\mathbf{1_M}$ were converted to 5-ethyl-4a-hydroxyriboflavins (giving poly-$\mathbf{2_HOH}$ and poly-$\mathbf{2_MOH}$, respectively) by a three-step polymer reaction through the corresponding 5-ethylriboflaviniums (poly-$\mathbf{2_H}$ and poly-$\mathbf{2_M}$, respectively) according to the method reported for small flavin compounds (Scheme 1 and Scheme S1 in the Supporting Information).[6f,7a,19] Purple-colored poly-**2** fractions were prepared by $NaBH_3CN$-mediated reductive ethylation of the poly-**1** fractions followed by oxidation with $NaNO_2$, and the riboflavinium units were successively converted to the corresponding 4a-hydroxy adducts via hydroxylation with a phosphate buffer at room temperature, thus producing poly-$\mathbf{2_HOH}$ and poly-$\mathbf{2_MOH}$. The resulting hydroxyriboflavin-containing polymers were further allowed to react with $HClO_4$, which resulted in the transformation back into the corresponding riboflavinium cations via dehydroxylation, affording poly-$\mathbf{2_H}$ and poly-$\mathbf{2_M}$, respectively (Scheme 1).[5,19a] The riboflavinium cations are versatile intermediates as biomimetic models of FADMO and also as organocatalysts for the H_2O_2-mediated oxidation of sulfides and amines.[3] In the same way, the corresponding model compounds model-**2** and model-**2OH** were also prepared for comparison (Scheme 2).

Figure 3 shows absorption and CD titrations of (A) poly-$\mathbf{2_MOH}$ and (B) model-**2OH** with increasing amounts of aqueous $HClO_4$ (60%) in CH_3CN. The addition of $HClO_4$ to a

Scheme 2. Synthesis of Model-2 and Model-2OH

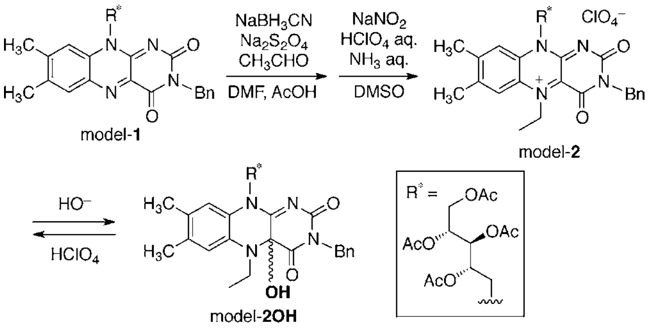

poly-2_M**OH** solution in CH_3CN caused a gradual and significant red shift of 254 nm in λ_{max} with clear isosbestic points at 298 and 380 nm in the absorption, reaching a constant pattern in the presence of 1 equiv of $HClO_4$. The solution color changed from pale yellow to purple, resulting from the generation of the conjugated flavinium cation species, poly-2_M. A similar dramatic change in the absorption was also observed for model-**2OH**, indicating that the conversion of the 4a-hydroxyriboflavin residues to the cationic species by dehydroxylation readily occurs, is independent of the MW, and is almost completed by 1 equiv of $HClO_4$. Interestingly, poly-2_M exhibited intense Cotton effects at around 290, 420, and 610 nm corresponding to the flavinium cation chromophores, whose intensities synchronously increased with increases in the amounts of $HClO_4$, whereas model-**2** showed negligible Cotton effects in the same regions, despite the fact that its absorption spectrum is almost identical to that of poly-2_M, demonstrating a remarkable difference in the chiroptical properties of the polymer and monomeric model-**2**.[20] The noticeable enhancement of the Cotton effects for poly-2_M compared with the weak CD for model-**2** suggests the formation of supramolecular aggregates of the poly-2_M backbones, which will be discussed later.

After the conversion of poly-2_M**OH** to poly-2_M with $HClO_4$ (1 equiv), the addition of Et_3N (1 equiv) to the poly-2_M solution regenerated the original poly-2_M**OH**, as revealed by the complete recovery of the absorption and CD spectra. As a result, the chiroptical properties of the polymers can be reversibly switched upon the alternative addition of acid and base (Figure S8 in the Supporting Information), which may enable the present 5-ethylriboflavin-containing polymers (poly-**2** and poly-**2OH**) to detect and sense the chirality of acids and bases by taking advantage of this chiroptical molecular switching behavior.[21]

Structure of Poly-2 Aggregates. To propose a possible structure for chiral poly-**2** in solution, the 2D nuclear Overhauser effect spectroscopy (NOESY) spectrum of poly-2_M was recorded in CD_3CN (Figure 4B and Figures S12 and S13 in the Supporting Information).[22] Several intermolecular NOE cross-peaks between the e and e′ protons of the ribityl groups and the 5-ethyl (x and y) and aromatic protons (a) were observed, whereas model-**2** showed no intermolecular NOE cross-peaks, as anticipated (Figures S17−S20 in the Supporting Information). In addition, the neutral poly-1_M did not show apparent intermolecular NOE cross-peaks between the riboflavin moieties (Figures S9 and S10 in the Supporting Information), in contrast to the cationic poly-2_M, probably because poly-1_M could not form such intermolecular contacts extensively enought to be detectable on the NMR time scale; the cationic poly-2_M chains may stack more efficiently than the neutral poly-1_M chains through electrostatic interactions assisted by oppositely charged counterions.

On the basis of these NOE results along with the CD data, a possible model for the interstrand-stacked poly-**2** structure can be proposed.[23] We assume that the poly-2_M chains most likely self-assemble to form a π-stacked duplexlike structure in such a way that the planar flavin repeating units stack face-to-face and the bulky ribityl groups are oriented antiparallel to each other to avoid steric repulsion, as illustrated in Figure 4A. The poly-**2** duplex may be loosely twisted clockwise or counterclockwise, accounting for the observation that poly-**2** exhibited extraordinarily intense Cotton effects in the flavinium chromophore regions. Hence, model-**2** showed negligible CD in the same regions. It has been reported that analogous riboflavin and flavin derivatives have a tendency to form similar face-to-face π-stacked structures in crystals.[25] If this is the case, there are two possible geometries for the stacking interactions. In the first of these, the flavin rings could intermolecularly stack in a regular

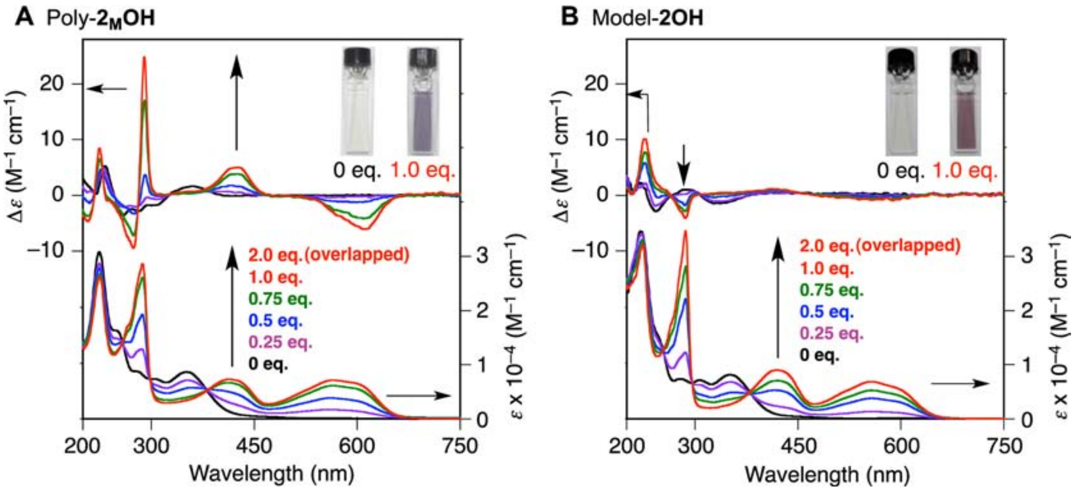

Figure 3. CD and absorption spectral changes of (A) poly-2_M**OH** and (B) model-**2OH** in CH_3CN (0.5 mM) in the presence of increasing amounts of $HClO_4$ (0, 0.25, 0.5, 0.75, 1.0, and 2.0 equiv) at ca. 25 °C. The insets show the color changes of poly-2_M**OH** and model-**2OH** in CH_3CN before and after the addition of $HClO_4$ (1.0 equiv).

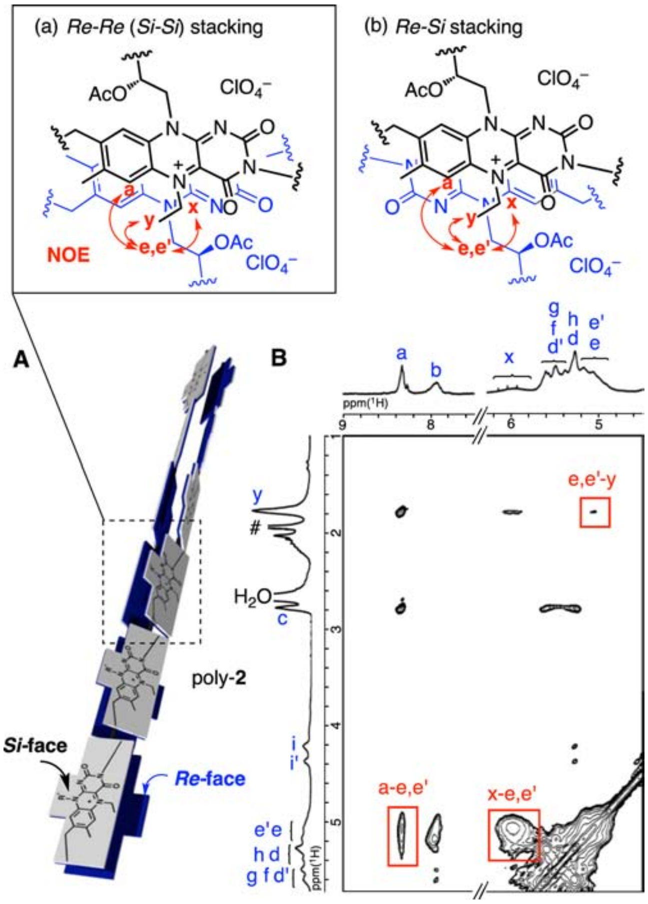

Figure 4. (A) Plausible interstrand face-to-face π-stacked structures for supramolecularly assembled, one-directionally twisted poly-**2**. (B) Partial NOESY spectrum of poly-$\mathbf{2_M}$ in CD_3CN at 25 °C; mixing time =200 ms. The peak were assigned on the basis of the 2D correlation spectroscopy (COSY) and NOESY spectra of model-**2** (see Figures S14−S20 in the Supporting Information).

way with the same *Re* (or *Si*) faces stacked with each other and the opposite *Si* (or *Re*) faces of each flavin ring efficiently open-surfaced [Figure 4A(a)]. The other possible geometry would involve *Re*−*Si* stacking interactions between the interstrand flavin rings [Figure 4A(b)]. At present, we are unable to distinguish the geometries [*Re*−*Re* (*Si*−*Si*) stacking vs *Re*−*Si* stacking] because of the lack of NOE cross-peaks between the riboflavin residues for unambiguous assignments, although the *Re*−*Re* (*Si*−*Si*) stacking may be predominant on the basis of the results for asymmetric oxidation catalyzed by poly-$\mathbf{2_M}$ (see below).

Diastereoselective Hydroxylation of Poly-2 and Model-2. Nucleophilic addition of hydroxide anions to the flavinium cation units of model-**2** and poly-**2** to afford the corresponding 4a-hydroxy adducts (model-**2OH** and poly-**2OH**, respectively) generates new stereogenic centers at the 4a-positions, thereby giving the (*R*)- and (*S*)-4a-hydroxy diastereomers. It was anticipated that one of the diastereomers could be formed diastereoselectively via induction by the optically active ribityl pendant groups. The formation of diastereomers of model-**2OH** was first elucidated by ^{1}H NMR and HPLC analyses. Figure 5A,B shows the ^{1}H NMR spectra of model-**2OH** and model-**2** derived from model-**2OH** (Scheme 2), respectively, as measured in CD_3CN. The ^{1}H NMR spectra of model-**2** gave simple peaks assigned as shown in Figure 5B and Figure S21B in the Supporting Information. In contrast, model-**2OH** showed two sets of peaks attributed to a diastereomeric pair (isomers A and B), and the diastereomeric excess (de) was estimated to be 8% (Figure 5A and Figure S21A) (for the peak assignments, see Figures S22−S25 in the Supporting Information). Further concrete evidence was obtained by HPLC analysis, as model-**2OH** was successfully separated into its diastereomers using a chiral column (Chiralpak IB, Daicel Co., Ltd.) with 1:1 (v/v) *n*-hexane/$CHCl_3$ as the eluent (Figure 5E); the de value was determined to be 9%, in good agreement with that estimated by the ^{1}H NMR analysis. We note that this is the first example of the separation of diastereomers of 4a-hydroxyriboflavin derivatives.

The ^{1}H NMR spectra of poly-$\mathbf{2_M}$**OH** and poly-$\mathbf{2_M}$ derived from poly-$\mathbf{2_M}$**OH** were also measured in CD_3CN (Figure 5C,D, respectively). Although the peaks became broadened, the resonance for the aromatic protons b of poly-$\mathbf{2_M}$**OH** split into two peaks (b_{major} and b_{minor}) with an integral ratio of 84:16 (Figure 5C). On the basis of the peak assignments using 2D NOESY measurements (Figures S27 and S28 in the Supporting Information) together with the fact that the same aromatic protons of the higher-MW poly-$\mathbf{2_H}$**OH** also split into two peaks with an integral ratio of 82:18 (Figure S26 in the Supporting Information), these two peaks could be assigned to the diastereomers derived from the 4a-hydroxyriboflavin units, with the contribution from the end groups of poly-**2OH** being negligibly small. Consequently, poly-$\mathbf{2_M}$**OH** and poly-$\mathbf{2_H}$**OH** were formed with 68 and 64% de, respectively, as estimated by NMR analysis; these de values are remarkably higher than that of model-**2OH** (8−9%). The intriguing enhancement of the diastereoselectivity observed for poly-**2** can be rationally explained on the basis of the supramolecularly stacked duplex structure of poly-**2** with an excess twist sense, as proposed in Figure 4A: one of the planar riboflavinium faces (*Re* or *Si*) is completely blocked via the favored face-to-face (*Re*−*Re* or *Si*−*Si*) π-stacking [Figure 4A(a)], allowing the hydroxide anion to be attacked only from the opposite open (*Si* or *Re*) face and thus preferentially producing the (*S*)- or (*R*)-4a-hydroxy adducts in poly-**2OH** with a relatively high diastereoselectivity.[26]

Enantioselective H_2O_2-Mediated Oxidation of Sulfides Catalyzed by Cationic Riboflavin-Containing Poly-2 and Its Model Monomer. We next applied the cationic riboflavin-containing polymer poly-**2** and its model monomer model-**2** as asymmetric organocatalysts for the biomimetic oxidation of sulfides with H_2O_2.[5,6a,b,e,h,i,l−r,t,7b] Flavinium cations have been reported to act as useful intermediates in oxidations of sulfides and Baeyer−Villiger reactions in the presence of H_2O_2; they generate the corresponding 4a-hydroperoxyflavins in situ via nucleophilic addition of H_2O_2, which are real active species for the monooxygenation of sulfides and cyclobutanones, respectively.[27] We anticipated from the diastereoselective hydroxylation results for poly-**2** that the riboflavinium cation units of poly-**2** having the supramolecularly twisted helical structure with excess one-handedness would also be diastereoselectively converted into one of the 4a-hydroperoxyriboflavin diastereomers (poly-**2OOH**) in the presence of H_2O_2, thus catalyzing the asymmetric oxidation of sulfides through the catalytic cycle shown in Scheme 3. The poly-**2OOH** generated in situ via mediation by H_2O_2 enantioselectively oxidizes sulfides to yield optically active sulfoxides along with the corresponding 4a-hydroxyriboflavin (poly-**2OH**), which undergoes dehydration to regenerate cationic poly-**2** to complete the catalytic cycle.

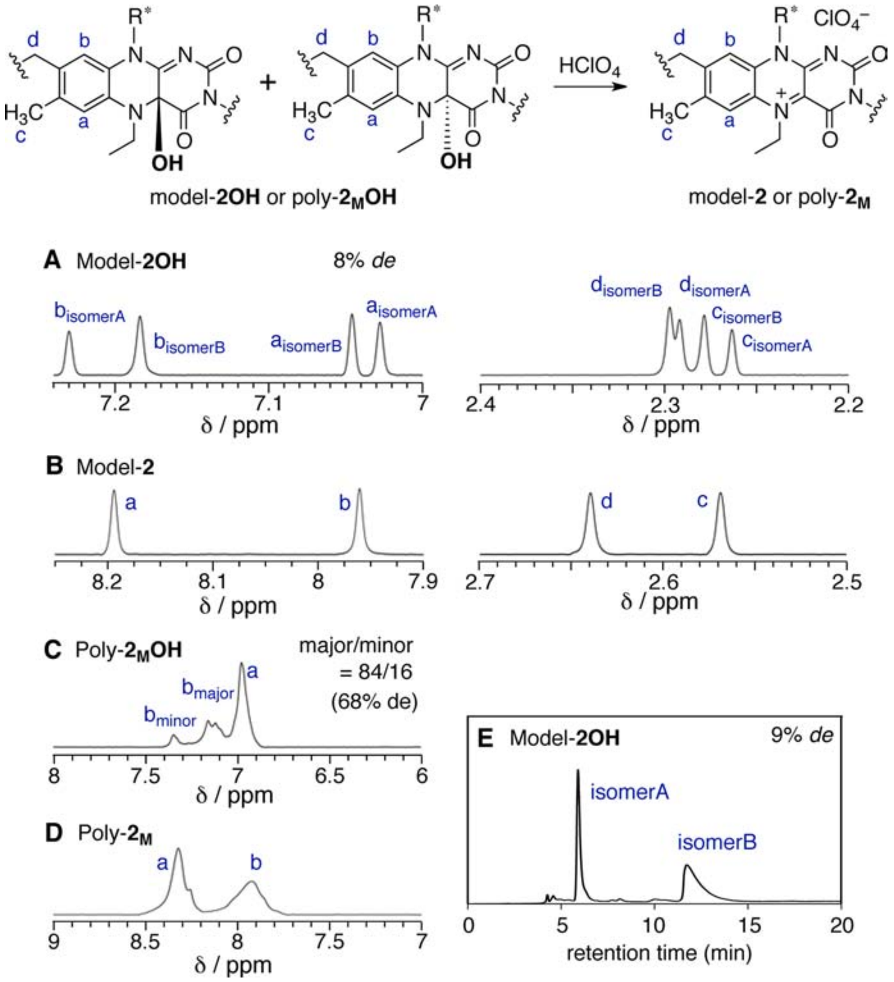

Figure 5. Partial ^{1}H NMR spectra of (A) model-**2OH**, (B) model-**2** prepared in situ from model-**2OH** by addition of $HClO_4$ (1 equiv), (C) poly-$\mathbf{2_M}$**OH**, and (D) poly-$\mathbf{2_M}$ derived from poly-$\mathbf{2_M}$**OH** by addition of $HClO_4$ (1 equiv) in CD_3CN. (E) HPLC trace of model-**2OH** using a Daicel Chiralpak IB column [1:1 (v/v) *n*-hexane/$CHCl_3$, 304 nm, 1 mL/min].

Scheme 3. Reaction Mechanism of H_2O_2-Mediated Asymmetric Oxidation of Sulfides Catalyzed by Poly-2

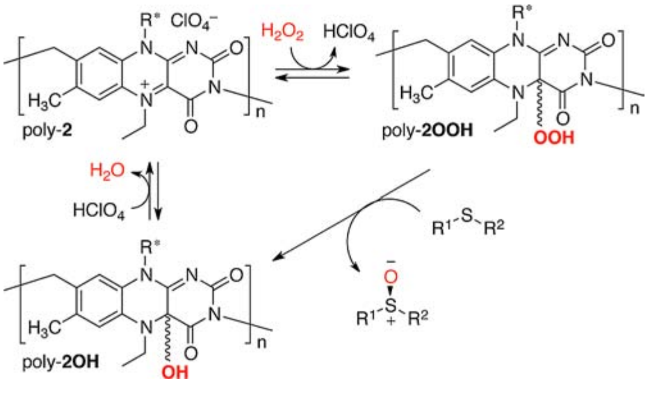

Table 1 summarizes the results for the asymmetric oxidation of methyl *p*-tolyl sulfide in CH_3CN and THF using poly-$\mathbf{2_M}$ or the corresponding monomeric model-**2** as the organocatalyst at −40 °C.[28] The H_2O_2-mediated asymmetric oxidation proceeded in the presence of poly-$\mathbf{2_M}$ or model-**2** in CH_3CN at −40 °C, producing (*S*)-methyl *p*-tolyl sulfoxide with 20 and 11% ee, respectively (Table 1, entries 1 and 2), demonstrating a relatively higher enantioselectivity with poly-$\mathbf{2_M}$ than with the monomeric model-**2**. The enantioselectivity observed in the asymmetric oxidation may be closely correlated to the stereochemistry (diastereoselectivity) of the active species, poly-$\mathbf{2_M}$**OOH** or model-$\mathbf{2_M}$**OOH**, catalytically generated during the reaction. However, it was difficult to estimate their de values using NMR analysis because of their labile characteristics in solution. We then performed the hydroxylation reaction of cationic poly-$\mathbf{2_M}$ and model-**2** using $Me_4N^+OH^-$ as a nucleophile in CD_3CN at −40 °C to obtain the corresponding 4a-hydroxy adducts, poly-$\mathbf{2_M}$**OH** and model-**2OH**, respectively, and their de values were estimated from their ^{1}H NMR spectra to be 66 and 29%, respectively (Figure S29A,B in the Supporting Information), and a value of 28% de was obtained for model-**2OH** by chiral HPLC analysis (Figure S29C in the Supporting Information) in a similar way as already mentioned. As a result, a good correlation was realized between the enantioselectivities of the asymmetric oxidations catalyzed by poly-$\mathbf{2_M}$ and model-**2** and the de values of the corresponding 4a-hydroxy adducts: poly-$\mathbf{2_M}$ afforded a higher enantioselectivity than model-**2** and possessed a higher de value.

In THF, poly-$\mathbf{2_M}$ gave a higher enantioselectivity (60% ee) than in CH_3CN in spite of the relatively lower catalyst loading, and the enhancement of the enantioselectivity relative to model-**2** was also observed for the asymmetric oxidations of other sulfides, such as methyl 2-naphthyl sulfide and 2-phenyl-

Table 1. Asymmetric Oxidations of Sulfides Catalyzed by Model-2 or Poly-2_M[a]

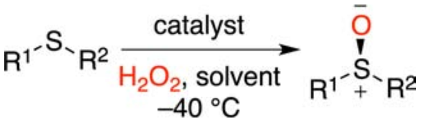

entry	substrate	product	catalyst	solvent	yield (%)[b]	*ee* (%)[c]
1[d]	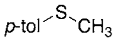	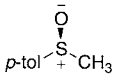	poly-2_M (50 mol%)	CH_3CN	70	20 (*S*)
2[d]			model-2 (50 mol%)	CH_3CN	62	11 (*S*)
3			poly-2_M (5 mol%)	THF	39	60 (*S*)
4			model-2 (5 mol%)	THF	28	30 (*S*)
5	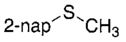	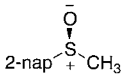	poly-2_M (5 mol%)	THF	40	42 (*S*)
6			model-2 (5 mol%)	THF	22	28 (*S*)
7	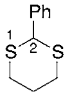	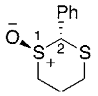	poly-2_M (5 mol%)	THF	66	13 (1*R*,2*R*) (>99% *de*)
8			model-2 (5 mol%)	THF	61	2 (1*R*,2*R*) (>99% *de*)

[a]Conditions: sulfide (0.1 M), model-2 or poly-2_M (5 mol %), and 30% aqueous H_2O_2 in solvent at −40 °C under N_2. [b]Isolated yields. [c]Determined by chiral HPLC. [d]The concentration of sulfide was 0.02 M.

1,3-dithiane (Table 1, entries 3−8).[29,30] Although the observed enantioselectivities of up to 60% ee were modest, the noticeable enhancement of the enantioselectivity over the monomeric counterpart clearly revealed that the supramolecular chirality induced in the riboflavin-containing polymers seemed to play an important role in the present H_2O_2-mediated asymmetric oxidation of sulfides.

It still remains unclear whether it is the (*R*)- or (*S*)-4a-hydroperoxy diastereomer (poly-**2_MOOH**) that is preferentially generated. However, on the basis of the fact that (*S*)-sulfoxides were enantioselectively produced with catalysis by poly-**2_MOOH** generated during the reaction and the plausible stacked structure of poly-**2_M** in Figure 4A, we propose a transition state model to account for the obtained asymmetric induction in the present enantioselective oxidation reaction (Figure 6). It can be assumed that poly-**2_M** may predominantly form a *Re*−*Re*-stacked duplex [Figure 4A(a)], to which the nucleophilic addition of H_2O_2 takes place from the opposite open *Si* face, thus generating the (*S*)-4a-hydroperoxy adduct (poly-**2_MOOH**). The sulfide substrate approached the hydroperoxy species in such a way that the phenyl ring of the substrate favorably interacts with the aromatic group of poly-**2_MOOH** via hydrophobic *π*-stacking, giving the (*S*)-sulfoxide.

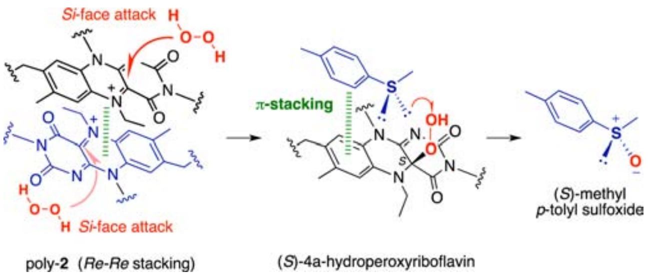

Figure 6. Possible transition state model for the asymmetric oxidation of sulfides by poly-**2_MOOH** possessing the (*S*)-4a-hydroperoxy configuration, which is generated in situ from the *Re*−*Re*-stacked poly-2_M duplex with an open *Si* face.

Vapochromic Behavior of Cationic Riboflavin-Containing Polymer Films upon Exposure to Amine Vapors. Vapochromic materials, which show drastic color changes upon exposure to volatile organic vapors, have attracted much attention because of their application to chemical sensing.[31] In particular, optical sensors that enable the selective detection of amines in solution have been studied extensively because of its importance in environmental and industrial monitoring, medical diagnosis, and quality control of food.[32] However, colorimetric sensory materials that selectively detect primary, secondary, and tertiary amine vapors by giving rise to color changes are quite limited,[33,34] whereas fluorescence sensors for amine vapors have been successfully developed.[35] We found that poly-**2** in the film state exhibits a rapid and reversible colorimetric response to primary and secondary amine vapors, thus enabling the direct visual detection of the amines (Table 2). The poly-**2_M** was readily processed into homogeneous films by drop-casting of its CH_3CN solution onto a thin glass plate. When a poly-**2_M** film was exposed to 2-propylamine vapor, the color of the film spontaneously changed from purple to yellow within 5 s (Table 2, entry 1). Exposure to other secondary and primary amine vapors resulted in similar color changes (entries 3−6). In sharp contrast, no vapochromic response was observed even after 1 h when the films were exposed to tertiary amine, ether, ester, amide, alcohol, and thiol vapors (entries 7−12). This specific and rapid vapochromic behavior toward secondary and primary amines can be explained by the nucleophilic and basic characteristics of the amines, which promote the formation of the corresponding 4a-amine adducts (poly-**2_MN**) and ammonium perchlorate.[36] Alcohols and thiols are also weak nucleophiles, but their 4a-adduct formations cannot be completed because of their lack of basicity, which prevents trapping of the in situ-generated perchloric acid (entries 11 and 12). This is supported by the fact that a vapochromic response was observed upon exposure to a mixture of the vapors of nucleophilic butanethiol and basic Et_3N for 1 h (entry 13), whereas the uses of Et_3N or butanethiol vapor separately resulted in no color change (entries 7 and 12).

Because the *π*-conjugated flavinium cation is changed to the nonconjugated 4a-amine adduct, the purple color due to the flavinium cation changes to yellow. The resulting yellow polymer films of poly-**2_MN** could be converted back to the original purple poly-**2_M** films through elimination of the amines by the treatment with diethyl ether containing $HClO_4$, and the

Table 2. Vapochromic Behavior of Poly-2_M Films upon Exposure to Various Organic Vapors[a]

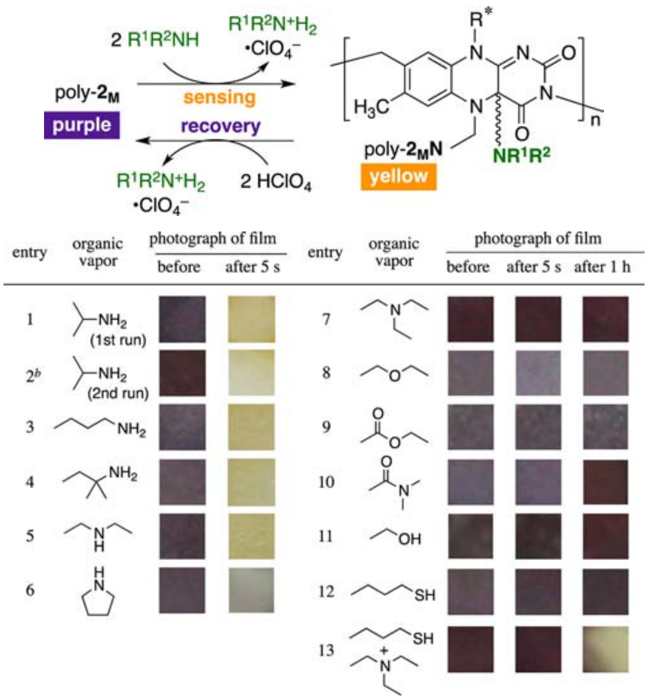

[a]Poly-2_M films drop-cast on thin glass plates were exposed to organic vapors at room temperature for the indicated times. [b]The poly-2_M film recovered after the first run (entry 1) by washing with aqueous $HClO_4$ in diethyl ether was reused.

recovered purple polymer films could be reused for further sensing of 2-propylamine (Table 2, entry 2). The absorption spectra of a poly-2_M film before and after the exposure to 2-propylamine vapor were then measured (Figure 7A). The absorption spectral pattern of the film was drastically changed upon treatment with the amine vapor, and the characteristic absorption peaks due to the conjugated flavinium cation units of poly-2_M (400−700 nm) almost completely disappeared within 5 s as a result of the nucleophilic addition of the amine to poly-2_M (Figure 7A), which was confirmed by the ^{1}H NMR spectral changes of poly-2_M in CD_3CN (Figure S30 in the Supporting Information). The addition of 2-propylamine resulted in a change in the ^{1}H NMR spectral pattern accompanied by the appearance of new peaks attributed to the formation of poly-$\mathbf{2_MN}$ and 2-propylammonium perchlorate. We further measured the absorption spectra of the samples used for the ^{1}H NMR measurements after dilution with CH_3CN (Figure 7B). The absorption spectral changes of poly-2_M in solution before and after the addition of 2-propylamine were almost identical to those observed in the film state, indicating that the conversion from poly-2_M to poly-$\mathbf{2_MN}$ in the film state definitely occurred upon exposure to 2-propylamine. These results suggest that the riboflavinium-containing polymers may be a novel and promising class of materials for rapid sensing of basic organic compounds in the solid state that could be visualized with the naked eye.

CONCLUSION

We have successfully synthesized the first optically active polymer composed almost entirely of the riboflavin residue as the main chain (poly-**1**) starting from commercially available riboflavin in three steps. The riboflavin residues of poly-**1** were converted to the corresponding 5-ethylriboflavinium cations to give poly-**2**, which further self-assembled to form a supramolecularly twisted, duplexlike helical structure with excess one-handedness through intermolecular face-to-face π-stacking of the riboflavinium units, as revealed by the absorption, CD, and NMR spectra. Poly-**2** catalyzed the H_2O_2-mediated asymmetric organocatalytic oxidation of sulfides with enantioselectivities of up to 60% ee, which is much higher than that catalyzed by the monomeric counterpart (30% ee). This remarkable enhancement of the enantioselectivity of poly-**2** relies on its helically twisted π-stacked structure, which most probably assists in the generation of the oxidatively active 4a-hydroperoxyflavins (poly-**2OOH**) in a diastereoselective manner. As a result of the reactive characteristics of the riboflavinium cations, poly-**2** showed a rapid and reversible

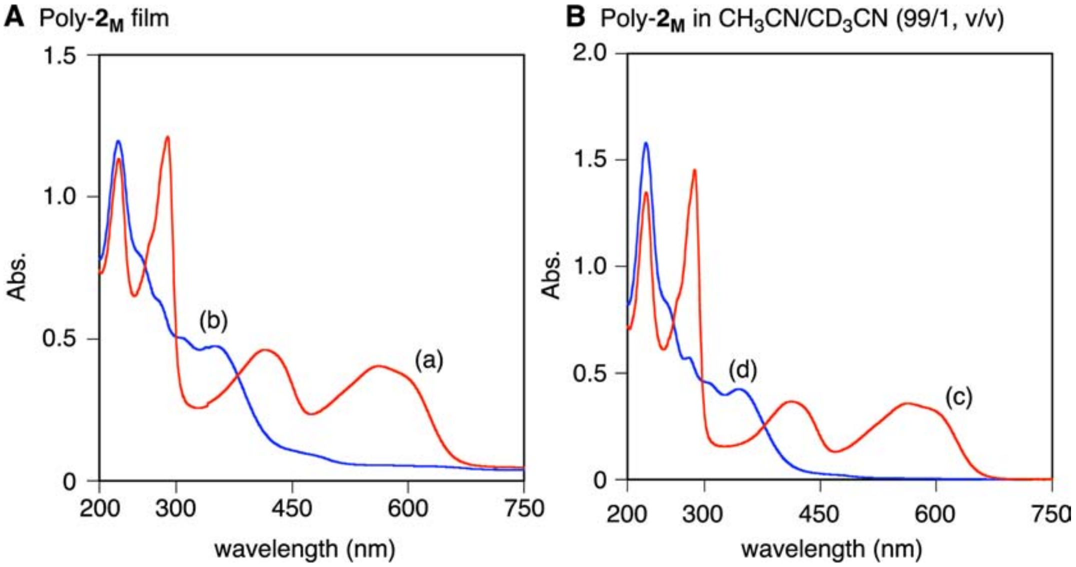

Figure 7. Absorption spectra of (A) a poly-2_M film (a) before and (b) after exposure to 2-propylamine vapor for 5 s and (B) poly-2_M in 99:1 (v/v) CH_3CN/CD_3CN (0.5 mM) in the (c) absence and (d) presence of 2 equiv of 2-propylamine.

colorimetric response to primary and secondary amine vapors in the film state, leading to the direct visual detection of the amines. The present study implies that optically active riboflavin-containing polymers will be a novel class of promising green asymmetric organocatalysts and could be applicable as chiral materials not only for sensing the chirality of chiral amines as well as single-walled carbon nanotubes[37] but also for separating enantiomers when used as a chiral stationary phase in liquid chromatography.[38]

■ ASSOCIATED CONTENT

Ⓢ Supporting Information

Full experimental details of the synthesis and ^{1}H NMR, COSY, NOESY, ROESY, CD, and absorption measurements of polymers and model compounds, asymmetric oxidation of sulfides, and vapochromic behavior. This material is available free of charge via the Internet at http://pubs.acs.org.

■ AUTHOR INFORMATION

Corresponding Author

yashima@apchem.nagoya-u.ac.jp

Notes

The authors declare no competing financial interest.

■ ACKNOWLEDGMENTS

This work was supported in part by a Grant-in-Aid for Scientific Research (S) (to E.Y.) and a Grant-in-Aid for Young Scientists (B) (to H.I.) from the Japan Society for the Promotion of Science (JSPS), the Kurata Memorial Hitachi Science and Technology Foundation (to H.I.), and the Global COE Program "Elucidation and Design of Materials and Molecular Functions" of the Ministry of Education, Culture, Sports, Science and Technology, Japan.

■ REFERENCES

(1) (a) Walsh, C. *Acc. Chem. Res.* **1980**, *13*, 148−155. (b) Bruice, T. C. *Acc. Chem. Res.* **1980**, *13*, 256−262. (c) Müller, F. *Chemistry and Biochemistry of Flavoenzymes*; CRC Press: Boston, 1991. (d) Massey, V. *Biochem. Soc. Trans.* **2000**, *28*, 283−296. (e) Mansoorabadi, S. O.; Thibodeaux, C. J.; Liu, H.-w. *J. Org. Chem.* **2007**, *72*, 6329−6342.

(2) (a) Choe, E.; Huang, R.; Min, D. B. *J. Food Sci.* **2005**, *70*, R28−R36. (b) Silva, E.; Edwards, A. M. *Flavins: Photochemistry and Photobiology*; Royal Society of Chemistry: Cambridge, U.K., 2006.

(3) (a) Imada, Y.; Naota, T. *Chem. Rec.* **2007**, *7*, 354−361. (b) Gelalcha, F. G. *Chem. Rev.* **2007**, *107*, 3338−3361.

(4) (a) Kemal, C.; Bruice, T. C. *Proc. Natl. Acad. Sci. U.S.A.* **1976**, *73*, 995−999. (b) Kemal, C.; Chan, T. W.; Bruice, T. C. *Proc. Natl. Acad. Sci., U.S.A.* **1977**, *74*, 405−409. (c) Ball, S.; Bruice, T. C. *J. Am. Chem. Soc.* **1979**, *101*, 4017−4019.

(5) Murahashi, S.-I.; Oda, T.; Masui, Y. *J. Am. Chem. Soc.* **1989**, *111*, 5002−5003.

(6) (a) Shinkai, S.; Yamaguchi, T.; Manabe, O.; Toda, F. *J. Chem. Soc., Chem. Commun.* **1988**, 1399−1401. (b) Murahashi, S.-I. *Angew. Chem., Int. Ed. Engl.* **1995**, *34*, 2443−2465. (c) Mazzini, C.; Lebreton, J.; Furstoss, R. *J. Org. Chem.* **1996**, *61*, 8−9. (d) Bergstad, K.; Bäckvall, J.-E. *J. Org. Chem.* **1998**, *63*, 6650−6655. (e) Minidis, A. B. E.; Bäckvall, J.-E. *Chem.—Eur. J.* **2001**, *7*, 297−302. (f) Murahashi, S.-I.; Ono, S.; Imada, Y. *Angew. Chem., Int. Ed.* **2002**, *41*, 2366−2368. (g) Imada, Y.; Iida, H.; Ono, S.; Murahashi, S.-I. *J. Am. Chem. Soc.* **2003**, *125*, 2868−2869. (h) Linden, A. A.; Krueger, L.; Bäckvall, J.-E. *J. Org. Chem.* **2003**, *68*, 5890−5896. (i) Linden, A. A.; Hermanns, N.; Ott, S.; Krueger, L.; Bäckvall, J.-E. *Chem.—Eur. J.* **2005**, *11*, 112−119. (j) Imada, Y.; Iida, H.; Naota, T. *J. Am. Chem. Soc.* **2005**, *127*, 14544−14545. (k) Imada, Y.; Iida, H.; Ono, S.; Masui, Y.; Murahashi, S.-I. *Chem.—Asian J.* **2006**, *1*, 136−147. (l) Linden, A. A.; Johansson, M.; Hermanns, N.; Bäckvall, J.-E. *J. Org. Chem.* **2006**, *71*, 3849−3853. (m) Baxova, L.; Cibulka, R.; Hampl, F. *J. Mol. Catal. A: Chem.* **2007**, *277*, 53−60. (n) Imada, Y.; Ohno, T.; Naota, T. *Tetrahedron Lett.* **2007**, *48*, 937−939. (o) Jurok, R.; Cibulka, R.; Dvorakova, H.; Hampl, F.; Hodacova, J. *Eur. J. Org. Chem.* **2010**, 5217−5224. (p) Zurek, J.; Cibulka, R.; Dvorakova, H.; Svoboda, J. *Tetrahedron Lett.* **2010**, *51*, 1083−1086. (q) Marsh, B. J.; Carbery, D. R. *Tetrahedron Lett.* **2010**, *51*, 2362−2365. (r) Mojr, V.; Herzig, V.; Budesinsky, M.; Cibulka, R.; Kraus, T. *Chem. Commun.* **2010**, *46*, 7599−7601. (s) Marsh, B. J.; Heath, E. L.; Carbery, D. R. *Chem. Commun.* **2011**, *47*, 280−282. (t) Mojr, V.; Budesinsky, M.; Cibulka, R.; Kraus, T. *Org. Biomol. Chem.* **2011**, *9*, 7318−7326. (u) Chen, S.; Hossain, M. S.; Foss, F. W. *Org. Lett.* **2012**, *14*, 2806−2809.

(7) (a) Imada, Y.; Iida, H.; Murahashi, S.-I.; Naota, T. *Angew. Chem., Int. Ed.* **2005**, *44*, 1704−1706. (b) Smit, C.; Fraaije, M. W.; Minnaard, A. J. *J. Org. Chem.* **2008**, *73*, 9482−9485. (c) Imada, Y.; Kitagawa, T.; Ohno, T.; Iida, H.; Naota, T. *Org. Lett.* **2010**, *12*, 32−35. (d) Imada, Y.; Iida, H.; Kitagawa, T.; Naota, T. *Chem.—Eur. J.* **2011**, *17*, 5908−5920. (e) Teichert, J. F.; den Hartog, T.; Hanstein, M.; Smit, C.; ter Horst, B.; Hernandez-Olmos, V.; Feringa, B. L.; Minnaard, A. J. *ACS Catal.* **2011**, *1*, 309−315.

(8) Optically active riboflavin derivatives were reported to promote some catalytic transformation reactions with no enantioselectivity (see ref 7), except for one precedent reported in a doctoral dissertation, in which a fully acetylated riboflavin derivative catalyzed the H_2O_2-mediated asymmetric oxidation of an aromatic sulfide in 1,2-dichloroethane at −20 °C to give the corresponding sulfoxide with 25% ee. See: Masui, Y. Ph.D. Thesis, Osaka University, Osaka, Japan, 1990.

(9) For examples of optically inactive flavin-containing polymers, see: (a) Bootsma, J. P. C.; Challa, G.; Müller, F. *J. Polym. Sci.: Polym. Chem. Ed.* **1984**, *22*, 705−719. (b) Challa, G.; van den Berg, H. J.; Schoo, H. F. M.; Blokzijl, W.; Pandit, U. K. *React. Polym.* **1989**, *10*, 219−230. (c) Schoo, H. F. M.; Challa, G. *Macromolecules* **1992**, *25*, 1633−1638. (d) Carroll, J. B.; Jordan, B. J.; Xu, H.; Erdogan, B.; Lee, L.; Cheng, L.; Tiernan, C.; Cooke, G.; Rotello, V. M. *Org. Lett.* **2005**, *7*, 2551−2554. (e) Jordan, B. J.; Cooke, G.; Garety, J. F.; Pollier, M. A.; Kryvokhyzha, N.; Bayir, A.; Rabani, G.; Rotello, V. M. *Chem. Commun.* **2007**, 1248−1250. (f) Patra, D.; Pagliuca, C.; Subramani, C.; Samanta, B.; Agasti, S. S.; Zainalabdeen, N.; Caldwell, S. T.; Cooke, G.; Rotello, V. M. *Chem. Commun.* **2009**, 4248−4250. (g) Subramani, C.; Yesilbag, G.; Jordan, B. J.; Li, X.; Khorasani, A.; Cooke, G.; Sanyal, A.; Rotello, V. M. *Chem. Commun.* **2010**, *46*, 2067−2069.

(10) For examples of optically active riboflavin-containing polymers, see: (a) Kamogawa, H. *J. Polym. Sci., Part A: Polym. Chem.* **1969**, *7*, 409−413. (b) Shinkai, S.; Yamada, S.; Kunitake, T. *Macromolecules* **1978**, *11*, 65−68. (c) Shinkai, S.; Ando, R.; Kunitake, T. *Biopolymers* **1978**, *17*, 2757−2760. (d) Spetnagel, W. J.; Klotz, I. M. *Biopolymers* **1978**, *17*, 1657−1668. (e) Shinkai, S.; Mori, K.; Kusano, Y.; Manabe, O. *Bull. Chem. Soc. Jpn.* **1979**, *52*, 3606−3610. (f) Iida, H.; Mizoguchi, T.; Oh, S.-D.; Yashima, E. *Polym. Chem.* **2010**, *1*, 841−848. (g) Thomas, T. P.; Choi, S. K.; Li, M.-H.; Kotlyar, A.; Baker, J. R., Jr. *Bioorg. Med. Chem. Lett.* **2010**, *20*, 5191−5194. (h) Witte, A. B.; Timmer, C. M.; Gam, J. J.; Choi, S. K.; Banaszak Holl, M. M.; Orr, B. G.; Baker, J. R., Jr.; Sinniah, K. *Biomacromolecules* **2012**, *13*, 507−516.

(11) Although a number of optically active polymers with main-chain chirality based on planar π-conjugated molecules derived from axially twisted binaphthyl derivatives[12a] and those bearing optically active side chains, such as poly(fluorene),[12b] poly(carbazole),[12c] and poly(dithienopyrrole),[12d] have been prepared, optically active polymers with main-chain chirality consisting of naturally occurring planar chiral molecules have hardly been reported.

(12) (a) Zhang, H.-C.; Pu, L. *Macromolecules* **2004**, *37*, 2695−2702. (b) Tang, H. Z.; Fujiki, M.; Sato, T. *Macromolecules* **2002**, *35*, 6439−6445. (c) Zhang, Z. B.; Motonaga, M.; Fujiki, M.; McKenna, C. E. *Macromolecules* **2003**, *36*, 6956−6958. (d) Vanormelingen, W.; Van den Bergh, K.; Verbiest, T.; Koeckelberghs, G. *Macromolecules* **2008**, *41*, 5582−5589.

(13) Walker, W. H.; Singer, T. P.; Ghisla, S.; Hemmerich, P. *Eur. J. Biochem.* **1972**, *26*, 279−289.

(14) (a) Sun, M.; Moore, T. A.; Song, P.-S. *J. Am. Chem. Soc.* **1972**, *94*, 1730−1740. (b) Heelis, P. F. *Chem. Soc. Rev.* **1982**, *11*, 15−39. (c) Choe, Y.-K.; Nagase, S.; Nishimoto, K. *J. Comput. Chem.* **2007**, *28*, 727−739.

(15) The reason for this weak concentration-dependent hyperchromic effect related to the poly-**1** structure in solution is not clear at present.

(16) It has been reported that flavins have a tendency to form π-stacked complexes in both solution and crystals. For examples in solution, see: (a) Sarma, R. H.; Dannies, P.; Kaplan, N. O. *Biochemistry* **1968**, *7*, 4359−4367. (b) Kotowycz, G.; Teng, N.; Klein, M. P.; Calvin, M. *J. Biol. Chem.* **1969**, *244*, 5656−5662. (c) Kainosho, M.; Kyogoku, Y. *Biochemistry* **1972**, *11*, 741−752. (d) Nakade, H.; Jordan, B. J.; Xu, H.; Han, G.; Srivastava, S.; Arvizo, R. R.; Cooke, G.; Rotello, V. M. *J. Am. Chem. Soc.* **2006**, *128*, 14924−14929. For examples in crystals, see: (e) von Glehn, M.; Norrestam, R. *Acta Chem. Scand.* **1972**, *26*, 1490−1502. (f) Porter, D. J. T.; Voet, D. *Acta Crystallogr.* **1978**, *B34*, 598−610. (g) Shinkai, S.; Kawanabe, S.; Kawase, A.; Yamaguchi, T.; Manabe, O.; Harada, S.; Nakamura, H.; Kasai, N. *Bull. Chem. Soc. Jpn.* **1988**, *61*, 2095−2102. (h) Ebitani, M.; In, Y.; Ishida, T.; Sakaguchi, K.; Flippen-Anderson, J. L.; Karle, I. L. *Acta Crystallogr.* **1993**, *B49*, 136−144. (i) Staab, H. A.; Kanellakopulos, J.; Kirsch, P.; Krieger, C. *Liebigs Ann.* **1995**, 1827−1836. (j) Reibenspies, J. H.; Guo, F.; Rizzo, C. J. *Org. Lett.* **2000**, *2*, 903−906. (k) Insinska-Rak, M.; Sikorska, E.; Herance, J. R.; Bourdelande, J. L.; Khmelinskii, I. V.; Kubicki, M.; Prukala, W.; Machado, I. F.; Komasa, A.; Ferreira, L. F. V.; Sikorski, M. *Photochem. Photobiol. Sci.* **2005**, *4*, 463−468. (l) Insinska-Rak, M.; Sikorska, E.; Bourdelande, J. L.; Khmelinskii, I. V.; Prukala, W.; Dobek, K.; Karolczak, J.; Machado, I. F.; Ferreira, L. F. V.; Dulewicz, E.; Komasa, A.; Worrall, D. R.; Kubicki, M.; Sikorski, M. *J. Photochem. Photobiol., A* **2007**, *186*, 14−23. (m) Chattopadhyay, P.; Nagpal, R.; Pandey, P. S. *Aust. J. Chem.* **2008**, *61*, 216−222. (n) Sikorska, E.; Hernando, J.; Bourdelande, J. L.; Khmelinskii, I.; Kubicki, M.; Komasa, A.; Prukala, D.; Sikorski, M. *Pol. J. Chem.* **2008**, *82*, 2141−2152.

(17) Rotello and co-workers reported that a chiral diaminopyridine−achiral flavin dyad formed a helically π-stacked self-assembly showing ICD in the flavin chromophore regions due to the induced supramolecular chirality in the achiral flavin units (see ref 16d). The formation of similar π-stacked aggregates with supramolecular chirality showing unique chiroptical properties has often been observed in π-conjugated optically active polymers such as polythiophenes. See: (a) Lemaire, M.; Delabouglise, D.; Garreau, R.; Guy, A.; Roncali, J. *J. Chem. Soc., Chem. Commun.* **1988**, 658−661. (b) Yashima, E.; Goto, H.; Okamoto, Y. *Macromolecules* **1999**, *32*, 7942−7945. (c) Goto, H.; Yashima, E. *J. Am. Chem. Soc.* **2002**, *124*, 7943−7949. (d) Wolffs, M.; Korevaar, P. A.; Jonkheijm, P.; Henze, O.; Feast, W. J.; Schenning, A. P. H. J.; Meijer, E. W. *Chem. Commun.* **2008**, 4613−4615. (e) Goto, H.; Yokochi, Y.; Yashima, E. *Chem. Commun.* **2012**, *48*, 3291−3293.

(18) Dynamic light scattering (DLS) measurements on poly-$\mathbf{1}_\mathrm{H}$ in DMF were attempted in order to obtain the hydrodynamic radius (R_h) of the polymer aggregates. However, estimation of the R_h value was difficult because the size of the aggregates may have been below the detection limit (~3 nm).

(19) (a) Ghisla, S.; Hartmann, U.; Hemmerich, P.; Müller, F. *Liebigs Ann. Chem.* **1973**, 1388−1415. (b) Mager, H. I. X.; Addink, R. *Tetrahedron* **1985**, *41*, 183−190.

(20) There were no significant differences in the CD and absorption spectra of poly-$\mathbf{2}_\mathrm{M}$ and poly-$\mathbf{2}_\mathrm{H}$ (Figure S5 in the Supporting Information). Poly-$\mathbf{2}_\mathrm{M}$ also showed similar temperature- and concentration-dependent CD spectral changes as observed for poly-$\mathbf{1}_\mathrm{M}$ (Figures S6 and S7, respectively, in the Supporting Information).

(21) For reviews of chiroptical molecular switches, see: (a) Feringa, B. L.; van Delden, R. A.; Koumura, N.; Geertsema, E. M. *Chem. Rev.* **2000**, *100*, 1789−1816. (b) Canary, J. W. *Chem. Soc. Rev.* **2009**, *38*, 747−756. (c) Klajn, R.; Stoddart, J. F.; Grzybowski, B. A. *Chem. Soc. Rev.* **2010**, *39*, 2203−2237.

(22) For more detailed results of NMR measurements, including the peak assignments for poly-$\mathbf{2}_\mathrm{M}$, model-**2**, poly-$\mathbf{2}_\mathrm{M}$**OH**, and model-**2OH** as well as poly-$\mathbf{1}_\mathrm{M}$, see Figures S9−S28 in the Supporting Information.

(23) We attempted to estimate the hydrodynamic radius of poly-$\mathbf{2}_\mathrm{H}$ in CH_3CN (5 mM) using DLS, but it was difficult because of the characteristic absorption of the poly-$\mathbf{2}_\mathrm{H}$ solution around the HeNe laser beam (632.8 nm). We then performed filtration experiments[24] on a poly-$\mathbf{2}_\mathrm{H}$ solution in CH_3CN (5 mM) using a membrane filter with a pore size of 20 nm; the absorption spectrum of the filtrate remained unchanged even after filtration, indicating that the formation of aggregates (>20 nm) could be excluded.

(24) (a) Goto, H.; Okamoto, Y.; Yashima, E. *Macromolecules* **2002**, *35*, 4590−4601. (b) Morino, K.; Maeda, K.; Yashima, E. *Macromolecules* **2003**, *36*, 1480−1486.

(25) For crystal structures of riboflavin derivatives, see refs 16h and 16l. For crystal structures of 10-alkylflavins, see refs 16e−g, 16i−k, 16m, and 16n.

(26) When poly-**2** forms an alternative *Re*−*Si*-stacked duplex structure [Figure 4A(b)], such a diastereoselective nucleophilic addition of the hydroxide anion may not be anticipated because both the *Re* and *Si* riboflavinium faces remain open, producing nondiastereoselective 4a-hydroxy adducts.

(27) Shinkai et al.[6a] and Murahashi et al.[6f] reported a cyclic flavinium and a C_2-symmetric bisflavinium with a planar chirality, in which one of the flavin faces was designed to be blocked by a cyclic cap moiety and the other flavin unit, resulting in efficient catalysis of the asymmetric oxidations of substrates with up to 65 and 74% ee, respectively.

(28) The reaction conditions were optimized with respect to the temperature and solvent. In diethyl ether, 4:1 (v/v) diethyl ether/CH_3CN, 4/1 (v/v) diethyl ether/THF, CH_3CN, and THF, the poly-$\mathbf{2}_\mathrm{M}$-catalyzed asymmetric oxidations of methyl *p*-tolyl sulfide produced (*S*)-methyl *p*-tolyl sulfoxide with 6, 17, 19, 20, and 60% ee, respectively. The enantioselectivity decreased with increasing temperature, whereas the reactions were completed faster at higher temperature; the poly-$\mathbf{2}_\mathrm{M}$-catalyzed asymmetric oxidation of methyl *p*-tolyl sulfide in CH_3CN at −40, −20, and 0 °C afforded the product with 20, 5.4, and 2.4% ee, respectively.

(29) This enantioselectivity of model-**2** for the asymmetric oxidation of methyl *p*-tolyl sulfide is comparable to that using an in situ-generated model-**2** analogue, as reported in ref 8.

(30) The de value for poly-$\mathbf{2}_\mathrm{M}$**OH** generated in situ from poly-$\mathbf{2}_\mathrm{M}$ with $\mathrm{Me_4N^+OH^-}$ in THF at −40 °C could not be determined because of the poor solubility of poly-$\mathbf{2}_\mathrm{M}$ in THF.

(31) For reviews of optical chemical sensors, see: (a) de Silva, A. P.; Gunaratne, H. Q. N.; Gunnlaugsson, T.; Huxley, A. J. M.; McCoy, C. P.; Rademacher, J. T.; Rice, T. E. *Chem. Rev.* **1997**, *97*, 1515−1566. (b) Bühlmann, P.; Pretsch, E.; Bakker, E. *Chem. Rev.* **1998**, *98*, 1593−1688. (c) Albert, K. J.; Lewis, N. S.; Schauer, C. L.; Sotzing, G. A.; Stitzel, S. E.; Vaid, T. P.; Walt, D. R. *Chem. Rev.* **2000**, *100*, 2595−2626. (d) Mohr, G. J. *Chem.—Eur. J.* **2004**, *10*, 1082−1090. (e) Thomas, S. W.; Joly, G. D.; Swager, T. M. *Chem. Rev.* **2007**, *107*, 1339−1386. (f) McDonagh, C.; Burke, C. S.; MacCraith, B. D. *Chem. Rev.* **2008**, *108*, 400−422.

(32) (a) Mohr, G. J.; Demuth, C.; Spichiger-Keller, U. E. *Anal. Chem.* **1998**, *70*, 3868−3873. (b) Fuji, K.; Tsubaki, K.; Tanaka, K.; Hayashi, N.; Otsubo, T.; Kinoshita, T. *J. Am. Chem. Soc.* **1999**, *121*, 3807−3808. (c) Reppy, M. A.; Cooper, M. E.; Smithers, J. L.; Gin, D. L. *J. Org. Chem.* **1999**, *64*, 4191−4195. (d) Mertz, E.; Zimmerman, S. C. *J. Am. Chem. Soc.* **2003**, *125*, 3424−3425. (e) Feuster, E. K.; Glass, T. E. *J. Am. Chem. Soc.* **2003**, *125*, 16174−16175. (f) Comes, M.; Marcos, M. D.; Martínez-Máñez, R.; Sancenón, F.; Soto, J.; Villaescusa, L. A.; Amorós, P.; Beltrán, D. *Adv. Mater.* **2004**, *16*, 1783−1786. (g) Greene, N. T.; Shimizu, K. D. *J. Am. Chem. Soc.* **2005**, *127*, 5695−5700. (h) Zhang, C.; Suslick, K. S. *J. Am. Chem. Soc.* **2005**, *127*, 11548−11549. (i) Jung, J. H.; Lee, S. J.; Kim, J. S.; Lee, W. S.; Sakata, Y.; Kaneda, T. *Org. Lett.* **2006**, *8*, 3009−3012. (j) Sasaki, S.-i.; Kotegawa, Y.; Tamiaki, H. *Tetrahedron Lett.* **2006**, *47*, 4849−4852. (k) Nelson, T. L.; O'Sullivan, C.; Greene, N. T.; Maynor, M. S.; Lavigne, J. J. *J. Am.

Chem. Soc. **2006**, *128*, 5640−5641. (l) Holthoff, E. L.; Bright, F. V. *Acc. Chem. Res.* **2007**, *40*, 756−767. (m) Montes-Navajas, P.; Baumes, L. A.; Corma, A.; Garcia, H. *Tetrahedron Lett.* **2009**, *50*, 2301−2304. (n) Bao, B.; Yuwen, L.; Zheng, X.; Weng, L.; Zhu, X.; Zhan, X.; Wang, L. *J. Mater. Chem.* **2010**, *20*, 9628−9634. (o) Körsten, S.; Mohr, G. J. *Chem.—Eur. J.* **2011**, *17*, 969−975. (p) Patze, C.; Broedner, K.; Rominger, F.; Trapp, O.; Bunz, U. H. F. *Chem.—Eur. J.* **2011**, *17*, 13720−13725 and references therein.

(33) (a) Kirchner, N.; Zedler, L.; Mayerhofer, T. G.; Mohr, G. J. *Chem. Commun.* **2006**, 1512−1514. (b) Liu, W.; Pink, M.; Lee, D. *J. Am. Chem. Soc.* **2009**, *131*, 8703−8707. (c) Lee, H. Y.; Song, X.; Park, H.; Baik, M.-H.; Lee, D. *J. Am. Chem. Soc.* **2010**, *132*, 12133−12144.

(34) Statistical analysis of colorimetric sensor arrays is also effective for the selective recognition of amine vapors. See: (a) Rakow, N. A.; Suslick, K. S. *Nature* **2000**, *406*, 710−713. (b) Rakow, N. A.; Sen, A.; Janzen, M. C.; Ponder, J. B.; Suslick, K. S. *Angew. Chem., Int. Ed.* **2005**, *44*, 4528−4532. (c) Bang, J. H.; Lim, S. H.; Park, E.; Suslick, K. S. *Langmuir* **2008**, *24*, 13168−13172.

(35) For examples of fluorescence sensors for amine vapors, see: (a) Charlesworth, J. M.; McDonald, C. A. *Sens. Actuators, B* **1992**, *8*, 137−142. (b) Thomas, S. W.; Swager, T. M. *Adv. Mater.* **2006**, *18*, 1047−1050. (c) Che, Y.; Yang, X.; Loser, S.; Zang, L. *Nano Lett.* **2008**, *8*, 2219−2223. (d) Liu, Y.; Wang, K.-R.; Guo, D.-S.; Jiang, B.-P. *Adv. Funct. Mater.* **2009**, *19*, 2230−2235. (e) Che, Y.; Zang, L. *Chem. Commun.* **2009**, 5106−5108. (f) He, C.; He, Q.; Deng, C.; Shi, L.; Zhu, D.; Fu, Y.; Cao, H.; Cheng, J. *Chem. Commun.* **2010**, *46*, 7536−7538. (g) Chow, C.-F.; Kong, H.-K.; Leung, S.-W.; Chiu, B. K. W.; Koo, C.-K.; Lei, E. N. Y.; Lam, M. H. W.; Wong, W.-T.; Wong, W.-Y. *Anal. Chem.* **2011**, *83*, 289−296. (h) Peterson, J. J.; Davis, A. R.; Werre, M.; Coughlin, E. B.; Carter, K. R. *ACS Appl. Mater. Interfaces* **2011**, *3*, 1796−1799. (i) Jiang, B.-P.; Guo, D.-S.; Liu, Y. *J. Org. Chem.* **2011**, *76*, 6101−6107. (j) Liu, X.; Zhang, X.; Lu, R.; Xue, P.; Xu, D.; Zhou, H. *J. Mater. Chem.* **2011**, *21*, 8756−8765. (k) Zhang, X.; Liu, X.; Lu, R.; Zhang, H.; Gong, P. *J. Mater. Chem.* **2012**, *22*, 1167−1172 and references therein.

(36) (a) Kim, J. M.; Bogdan, M. A.; Mariano, P. S. *J. Am. Chem. Soc.* **1993**, *115*, 10591−10595. (b) Hoegy, S. E.; Mariano, P. S. *Tetrahedron* **1997**, *53*, 5027−5046.

(37) (a) Ju, S.-Y.; Doll, J.; Sharma, I.; Papadimitrakopoulos, F. *Nat. Nanotechnol.* **2008**, *3*, 356−362. (b) Ju, S.-Y.; Kopcha, W. P.; Papadimitrakopoulos, F. *Science* **2009**, *323*, 1319−1323.

(38) (a) Okamoto, Y.; Yashima, E. *Angew. Chem., Int. Ed.* **1998**, *37*, 1020−1043. (b) Okamoto, Y.; Ikai, T. *Chem. Soc. Rev.* **2008**, *37*, 2593−2608. (c) Tamura, K.; Miyabe, T.; Iida, H.; Yashima, E. *Polym. Chem* **2011**, *2*, 91−98. (d) Miyabe, T.; Iida, H.; Yashima, E. *Chem. Sci.* **2012**, *3*, 863−867.